HHS Public Access

Author manuscript

Acad Radiol. Author manuscript; available in PMC 2018 August 01.

Published in final edited form as:

Acad Radiol. 2017 August ; 24(8): 941–946. doi:10.1016/j.acra.2016.08.023.

The Objective Identification and Quantification of Interstitial Lung Abnormalities in Smokers

Samuel Y. Ash, MD[a,*], **Rola Harmouche, PhD**[b,*], **James C. Ross, PhD**[b], **Alejandro A. Diaz, MD MPH**[a], **Gary M. Hunninghake, MD MPH**[a], **Rachel K Putman, MD**[a], **Jorge Onieva, MSc**[b], **Fernando J. Martinez, MD MS**[c], **Augustine M. Choi, MD**[c], **David A. Lynch, MD**[d], **Hiroto Hatabu, MD PhD**[e], **Ivan O. Rosas, MD**[a], **Raul San Jose Estepar, PhD**[b,†], and **George R. Washko, MD**[a,†] **for the COPDGene Investigators**

[a]Division of Pulmonary and Critical Care Medicine, Department of Medicine, Brigham and Women's Hospital, 75 Francis St., PBB, CA-3, Boston, MA 02115

[b]Laboratory of Mathematics in Imaging, Department of Radiology, Brigham and Women's Hospital, 1249 Boylston St., Boston, MA 02115

[c]Department of Medicine, Weil Cornell Medical College, 1300 York Avenue, New York, NY 10065

[d]Department of Radiology, National Jewish Health, 1400 Jackson St, A330, Denver, CO 80206

[e]Department of Radiology, Brigham and Women's Hospital, 75 Francis St., Boston, MA 02115

Abstract

Rationale and Objectives—Previous investigation suggests that visually detected interstitial changes in the lung parenchyma of smokers are highly clinically relevant and predict outcomes including death. Visual subjective analysis to detect these changes is time consuming, insensitive to subtle changes and requires training to enhance reproducibility. Objective detection of such changes could provide a method of disease identification without these limitations. The goal of this study was to develop and test a fully automated image processing tool to objectively identify radiographic features associated with interstitial abnormalities in the computed tomography scans of a large cohort of smokers.

Materials and Methods—An automated tool that uses local histogram analysis combined with distance from the pleural surface was used to detect radiographic features consistent with interstitial lung abnormalities in computed tomography scans from 2257 individuals from the

Corresponding Author: Samuel Y. Ash, MD, Division of Pulmonary and Critical Care Medicine, Brigham and Women's Hospital, 75 Francis St., PBB, CA-3, Boston, MA 02115, Tel: 857-307-0312, Fax: 617-582-6011, syash@partners.org.

*Both authors contributed equally to this work

†Both authors contributed equally to this work

Author contributions: Study concept and design: Ash, Harmouche, Ross, Estepar, Washko; Acquisition, analysis, or interpretation of data: All authors; Drafting of the manuscript: All authors; Intellectual Content: All authors; Statistical analysis: Ash, Diaz, Putman, Washko; Obtained funding: Washko, Estepar, Lynch, Hunninghake, Choi; Administrative, technical or material support: Ash, Harmouche, Ross, Onieva Onieva, Estepar; Study supervision: Washko, Estepar

Genetic Epidemiology of COPD study, a longitudinal observational study of smokers. The sensitivity and specificity of this tool was determined based on its ability to detect the visually identified presence of these abnormalities.

Measurements and Main Results—The tool had a sensitivity of 87.8% and a specificity of 57.5% for the detection of interstitial lung abnormalities, with a c-statistic of 0.82, and was 100% sensitive and 56.7% specific for the detection of the visual subtype of interstitial abnormalities called fibrotic parenchymal abnormalities, with a c-statistic of 0.89.

Conclusions and Relevance—In smokers, a fully automated image processing tool is able to identify those individuals who have interstitial lung abnormalities with moderate sensitivity and specificity.

Keywords Terms

Pulmonary Fibrosis; Idiopathic; CT Scanner; X-Ray; Pneumonia; Interstitial; Diffuse Parenchymal Lung Diseases; Cigarettes

Introduction

Interstitial lung diseases (ILD) such as idiopathic pulmonary fibrosis (IPF) have long been described based on clinical, radiographic and pathologic findings. However, there is a growing recognition that a broader definition is required to identify the early stages of ILD. (1) This has become increasingly important with the introduction of new therapies that slow, but do not reverse the progression of IPF, which is a progressive and frequently fatal disease. (2, 3) Interstitial lung abnormalities are radiographic precursor lesions to ILD, which themselves are associated with reduced total lung capacity, decreased exercise capacity, and increased mortality. (4–8) In populations at risk for ILD, such as smokers, the rate of interstitial lung abnormalities seen visually on computed tomography (CT) scans can be as high as 9.7%, but visual analysis alone may be insensitive to very early pathology and grading systems built using visual analysis may be inaccurate.(8–10)

Certain types of objective analysis of CT images, including densitometric and textural based approaches, have been shown to be sensitive for detecting ILD in patients at high risk, and have been found to correlate with pulmonary function and mortality in those with known ILD.(11–15) However, the role of objective CT as a screening tool for the detection of interstitial lung abnormalities in a large cohort of smokers is unknown.

We have developed an objective and fully automated method that uses the local histogram pattern of lung density proposed by Mendoza et al, but which in addition also incorporates the distance to the pleural surface to identify and quantify the volume of radiographic features consistent with interstitial lung abnormalities on CT imaging of 9501 smokers.(16) We hypothesized that the objective measurement of these interstitial radiographic features would accurately identify those individuals who have visually identified interstitial lung abnormalities, and may also identify those individuals who have the visually defined subtype of interstitial abnormalities called fibrotic parenchymal abnormalities.

Materials and Methods

Study Design and Image Acquisition

COPDGene is a longitudinal investigation focused on the epidemiologic and genetic risk factors for the development of chronic obstructive pulmonary disease (COPD) in smokers. 10,300 smokers were enrolled, and each underwent a protocolized study visit which included an extensive interview, volumetric high resolution CT scanning of the chest, and spirometric assessments of lung function. Smokers between the ages of 45 and 80 with at least a 10 pack year history of tobacco smoke exposure were eligible to enroll. Subjects were excluded if they had active lung diseases other than asthma or COPD. These exclusion criteria included the presence of ILD as determined by the visual review of CT scans by the COPDGene imaging core.(17)

Volumetric CT scans of the chest were performed at both maximal inflation and relaxed exhalation. Images were acquired with the following CT protocol: for General Electric (GE) LightSpeed-16, GE VCT-64, Siemens Sensation-16 and -64, and Philips 40- and 60-slice scanners with 120kVp, 200mAs, and 0.5s rotation time. Images were reconstructed using a standard algorithm at 0.625mm slice thickness and 0.625mm intervals for GE scanners; using a B31f algorithm at 0.625 (Sensation-16) or 0.75mm slice thickness and 0.5mm intervals for Siemens scanners; and using a B algorithm at 0.9mm slice thickness and 0.45mm intervals for Philips scanners.

All subjects who participated in COPDGene provided written informed consent, and the study was approved by the institutional review boards at all of the participating centers.

Objective CT Analysis

The objective detection and quantification of the volume of radiographic interstitial feature subtypes was performed using an approach similar to that which we designed for evaluating subtypes of emphysema, and which combines the attenuation properties of the local tissue and distance from the pleural surface.(18) First, segmentation of the lung parenchyma from the chest wall and surrounding structures was performed on the inspiratory scans using a fully automated approach which uses particles, thin plate splines and maximum a posteriori estimation. This method has been described previously and was implemented through the Chest Imaging Platform (http://acil.med.harvard.edu/chest-imaging-platform).(19)

In order to train the objective detection and quantification tool, two experts placed 33865 fiducials in 138 CT scans on radiologic features unique to each disease type. The training CT scans were randomly selected by subject identification number. The radiologic features included normal parenchyma, interstitial feature subtypes (reticular, honeycombing, centrilobular nodule, linear scar, nodular, subpleural line, ground glass), and emphysema subtypes (centrilobular and paraseptal). (Note that panlobular emphysema was not identified in the training cases likely because patients with alpha 1 antitrypsin disease were not represented in the cohort.) This was done to build a library of points to be used as tissue classifiers.

Regions of interest (ROI) consisting of 30 by 30 in-plane voxels centered about these training points were constructed to use as training data. For each ROI a feature vector was built consisting of a local density histogram obtained using kernel density estimation (KDE) and distance to the pleural surface. KDE is a non-parametric method used to estimate a probability distribution over the densitometry values in each region of interest by smoothing over the local histogram information. This is especially useful when a parametric distribution cannot be fit over the densitometry values. The estimated distribution ($\hat{f}$) as a function of densitometry value (x) was obtained by smoothing a normalized histogram of all patch samples (x_i) using a Gaussian kernel (K). The smoothing factor (h) is particularly useful due to the finite number of densitometry samples per patch. Higher values of h result in increased smoothing of the distribution and the optimal value for this factor was obtained using methods described previously.(16, 20)

$$\hat{f}(x) = \frac{1}{nh} + \sum_{i=1}^{\infty} K\left(\frac{x - x_i}{h}\right)$$

The final feature incorporated into the tissue vector was the distance from each ROI to the closest point on the pleural surface. This distance information is especially helpful for classifying conditions such as a subpleural line which are localized to the lung periphery.

After the training process was completed, de-novo regions of the CT scan were classified based on their similarity to the training data. The feature vectors consisting of histogram and distance features were extracted from each test region of interest and were compared to the features vectors of each region in the training data. For the comparison, the following metric that combines the L_1 norm between the local density histograms and a weighted difference between the distances to the chest wall was used:

$$\begin{aligned} &\text{Density Metric} \\ &= L_1(\text{training histogram},\ \text{test histogram}) + \beta \\ &\times L_1(\text{training distance},\ \text{test distance}) \end{aligned}$$

The weight (β) was determined by performing a Bayesian optimization using the Spearmint package.(21) Within this data set, an optimal weight of 0.026 was found. A k-nearest neighbor classification scheme was then used to select the label with the highest frequency from the 5 nearest training neighbors as determined by the distance metric.

The results of this objective analysis assigned a tissue subtype to every portion of the lung parenchyma and provided the volume of each tissue subtype. The total percentage of all of the interstitial lung features was then determined by combining the reticular, centrilobular nodule, linear scar, nodular, subpleural line, ground glass and honeycombing subtype volumes and dividing by the total volume of all subtypes including normal, interstitial and emphysematous. CT scans included in the training subset were not excluded from the primary analysis, but represented only 7.09% of the total number of CT scans analyzed. A secondary analysis which excluded individuals with CT scans included in the training subset was also performed.

Visual HRCT Analysis

The visual assessment of CT for interstitial lung abnormalities in subjects participating in COPDGene has been described previously and was performed in two stages.(5, 7) In stage 1, each CT was evaluated by three readers (one pulmonologist and two chest radiologists, two of whom were separate from the readers who placed fiducials for the objective analysis) using a sequential reading method.(7) Interstitial lung abnormalities were defined as non-dependent ground-glass or reticular abnormalities, diffuse centrilobular nodularity, nonemphysematous cysts, honeycombing, or traction bronchiectasis affecting more than 5% of any lung zone. Focal or unilateral ground-glass attenuation, focal or unilateral reticulation, and patchy ground glass abnormalities (present in less than 5% of the lung) were considered to be indeterminate findings. In stage 2 of the visual CT analysis, those subjects who had interstitial lung abnormalities were subcategorized into having one of four major radiographic subtypes. For the purposes of this particular study, only one of these subtypes was considered: fibrotic parenchymal abnormalities, the diagnosis of which was based on the presence of the following CT findings: bilateral ground glass opacities with irregular reticular opacities and traction bronchiectasis or bronchiolectasis, in the absence of significant honeycombing.(8)

Statistical Analysis

The percentage of interstitial features was evaluated both as a continuous and a binary variable. Receiver operating characteristic curves and the area under the curve were generated using logistic regression for the objective detection of visually defined interstitial abnormalities and for the objective detection of fibrotic parenchymal abnormalities. Subgroup analyses were performed in which those subjects who were visually categorized as having indeterminate evidence of interstitial abnormalities were excluded. The sensitivity, specificity, positive predictive value and negative predictive value for the objective detection of visually defined interstitial abnormalities and for the detection of visually defined fibrotic parenchymal abnormalities were calculated after dichotomizing subjects using a cut off of 5% of the lung volume occupied by objective interstitial features, i.e. those subjects with greater than 5% of their lung volume occupied by objective interstitial features were defined as having objective disease. All analyses were performed using SAS software, version 9.4 (SAS Institute. Cary, NC).

Results

Cohort

Of the 10300 study participants in COPDGene, 9501 (92%) had a CT scan available that could be successfully analyzed using the objective technique. Of these, visual analysis of CT was available for 2257 (24%). Summary statistics for the cohort are shown in Table 1.

Validation of the Objective Detection Algorithm

Validation was performed in three parts. First, in order to perform a small scale preliminary review of the method, we performed a visual inspection of the tissue classification on full CT volumes of 5 random subjects. This revealed a systematic over classification of

paraseptal emphysema as reported previously using the local histogram method.(18) We therefore removed the 205 paraseptal subtype regions from the training data. This resulted in regions previously classified as paraseptal emphysema being reclassified as either normal parenchyma or centrilobular emphysema. We next performed a leave-one-out validation on the 33660 remaining regions of interest, whereby at each iteration, one of the regions was selected as the testing data, and the remaining regions were selected to be part of the training data. This portion of validation was performed in two phases. The first phase was undertaken with aggregated features of emphysema and interstitial lung features. In this way a ROI in the lung was labeled as “normal”, “emphysema” or “interstitial”. This was done to generate a preliminary estimate of the overall ability our algorithm to differentiate disease subtypes. The average overall accuracy of the algorithm assessed in Phase 1 was 80.9% with an accuracy of 79.0% for the classification of “interstitial”. The second phase involved a leave-one-out validation with the non-aggregated subtypes. In this step the emphysema features, interstitial features (reticular, centrilobular nodule, linear scar, nodular, subpleural line, ground glass and honeycombing), and normal parenchyma were interrogated as unique patterns of disease. When examined by interstitial and emphysema subtype the overall average accuracy was 53.3%. Further review of the data illustrates that the accuracy of the algorithm was greater than 71% for honeycombing and greater than 78% for reticular changes, but only 12.9% for nodular changes and 12.4 for ground glass.

As expected, there was differential accuracy based on interstitial subtype due to differing numbers of fiducials per subtypes. For instance, while 5531 points were used to train for the reticular subtype, only 116 were used for the nodular subtype. This discrepancy in number of fiducials per tissue subtype was due to the visual prevalence of each feature in the training CTs. Also, the training data used for the leave-one-out validation included peripheral areas of normal parenchyma and disease, which was beneficial for the full volume classification but penalized leave-one-out accuracy.

Distribution ofObjective Interstitial Lung Features in the Cohort

The percentage of lung volume occupied by objectively identified interstitial features within each individual’s CT scan ranged from 0.567% to 45.1%, with a mean of 5.80%. The full distribution of the percentage of objective interstitial features in the cohort is shown in Figure 2, and a representative CT image showing the labeling of interstitial features is shown in Figure 3.

Objective Detection of Visually Defined Interstitial Lung Abnormalities

Objective interstitial lung features were found to have an area under curve (AUC) of the receiver operating characteristic (ROC) curve of 0.82 for the detection of visually defined interstitial lung abnormalities and an AUC 0.89 for the detection of visually defined fibrotic parenchymal abnormalities. When defined using the cutoff value of 5% lung volume occupied by objective interstitial lung features, the objective lung feature detector had a sensitivity of 87.8% and a specificity of 57.5% for visually defined interstitial lung abnormalities, and had a sensitivity of 100% and a specificity of 56.7% for visually defined fibrotic parenchymal abnormalities. Based on an observed prevalence of 6.91% for visually defined interstitial lung abnormalities and of 4.12% for the fibrotic parenchymal abnormality

subtype, the positive predictive and negative predictive values for the detection of interstitial abnormalities were 13.3% and 98.5 respectively, and for the detection of fibrotic parenchymal abnormalities were 9.03% and 100%. When subjects with indeterminate visual findings were excluded from the analysis, the detector was 87.8% sensitive and 72.6% specific for interstitial lung abnormalities with an AUC of 0.88, and was 100% sensitive and 70.6% specific for fibrotic parenchymal abnormalities with an AUC of 0.94.

When the individuals whose CT scans were in the training subset were excluded from the primary analysis the AUC for the detection interstitial abnormalities was 0.81, and the AUC for the detection of fibronodular abnormalities was 0.90. When both the training scans and those scans which were visually indeterminate were excluded, the AUC for the detection interstitial abnormalities was 0.87, and the AUC for the detection of fibronodular abnormalities was 0.94.

Discussion

In this study we found that the objective assessment of radiographic interstitial lung features in smokers using a fully automated method that involves local histogram analysis and the distance from the pleural surface can identify individuals with interstitial lung abnormalities.

Previous studies of the objective assessment of interstitial lung abnormalities and ILD have used semi-quantitative methods utilizing visual scoring systems, or have focused on the correlation of objective measures with specific visually defined tissue types, spirometry or other outcomes. And the majority of these studies have been done in subjects previously visually or pathologically identified as having interstitial disease.(12, 14, 15, 22–29) The role of objective radiographic analysis tools in identifying those with interstitial lung abnormalities in a large population is, however, less clear.

This led us to investigate the ability of our local histogram and distance based objective approach to identify and quantify radiographic features consistent with interstitial lung abnormalities from a large cohort of patients who are not known to have, and are at only mildly increased risk for, interstitial lung disease. Beyond its size and novel approach, additional strengths of our study include the relatively high area under the curve for the detection of both interstitial lung abnormalities and the fibrotic parenchymal visual subtype of interstitial abnormalities.

Our study does have several limitations. The most prominent is the discrepancy in prevalence between those with visually defined interstitial lung abnormalities (6.91%) and the prevalence of those had objectively defined interstitial lung features using our method (45.6%). We chose 5% objective interstitial features by volume because prior visual analyses had used this as a cut-off for the visual identification of interstitial lung abnormalities.(7) It should be noted that it is extremely unlikely that 45.6% of the population has early ILD. That said, the high negative predictive value of the tool suggests it may have a role as an objective screen for what is visually a relatively uncommon finding. In this way it would not replace visual interpretation of CT imaging, but rather provide automated and objective assistance in interpretation. In addition, based on this defined prevalence, as well as the

observation that fifty percent of subjects had a percentage of objective interstitial features of at least 4.65%, the objective interstitial lung features identified using this method are likely not just what are visually identified as interstitial lung abnormalities. Instead, it may be that while some of the patients with these features are those who have disease that is not yet discernible by visual inspection, others may represent an overlapping, but different group, such as those at risk for developing another smoking related disease in the future. In the latter scenario, these changes could be thought of as a possible marker of increased risk for cigarette related lung disease or of increased risk for other causes of smoking related mortality. It is also possible that some proportion of these findings are truly incidental. Further study will be needed to determine if this is the case, and to better identify the clinical characteristics of patients with these objective findings, what additional risk the findings may signify and what interventions might be available to reduce any such risk.

An additional limitation of this study relates to the exclusion of subjects with indeterminate scans in the secondary analysis. This was done for comparison with the visual literature, in which those subjects are often excluded. However, it should be noted that such a step would not be possible if the detector was used as a screening tool.

In conclusion, our study of the objective assessment of radiographic interstitial lung features in smokers has shown that an automated detector of interstitial lung features can identify individuals with interstitial lung abnormalities. Further study is needed to determine if these objective abnormalities are associated with spirometric values and clinical outcomes such as mortality.

Acknowledgments

Funding/Sponsor: This work was supported by NIH grants: 5-T32-HL007633-30 (Ash, Putman), R01-HL107246 (Washko, Estepar, Harmouche, Onieva Onieva), R01-HL116933 (Washko, Estepar, Ross, Harmouche, Onieva Onieva), R01-HL111024 (Hunninghake), P01-HL114501 (Choi, Rosas, Washko) and R01-HL089856 (Washko, Lynch, Estepar, Ross).

Abbreviations

CT	computed tomography
COPD	chronic obstructive pulmonary disease
GE	General Electric
ILD	interstitial lung disease
IPF	idiopathic pulmonary fibrosis
ROI	region of interest

References

1. Rosas IO, Dellaripa PF, Lederer DJ, Khanna D, Young LR, Martinez FJ. Interstitial lung disease: NHLBI Workshop on the Primary Prevention of Chronic Lung Diseases. Annals of the American Thoracic Society. 2014; 11(Suppl 3):S169–177. [PubMed: 24754826]

2. King TE Jr, Bradford WZ, Castro-Bernardini S, Fagan EA, Glaspole I, Glassberg MK, Gorina E, Hopkins PM, Kardatzke D, Lancaster L, Lederer DJ, Nathan SD, Pereira CA, Sahn SA, Sussman R, Swigris JJ, Noble PW. A phase 3 trial of pirfenidone in patients with idiopathic pulmonary fibrosis. The New England journal of medicine. 2014; 370:2083–2092. [PubMed: 24836312]

3. Richeldi L, du Bois RM, Raghu G, Azuma A, Brown KK, Costabel U, Cottin V, Flaherty KR, Hansell DM, Inoue Y, Kim DS, Kolb M, Nicholson AG, Noble PW, Selman M, Taniguchi H, Brun M, Le Maulf F, Girard M, Stowasser S, Schlenker-Herceg R, Disse B, Collard HR. Efficacy and safety of nintedanib in idiopathic pulmonary fibrosis. The New England journal of medicine. 2014; 370:2071–2082. [PubMed: 24836310]

4. Putman RK, Hatabu H, Araki T, et al. ASsociation between interstitial lung abnormalities and all-cause mortality. Jama. 2016; 315:672–681. [PubMed: 26881370]

5. Washko GR, Hunninghake GM, Fernandez IE, Nishino M, Okajima Y, Yamashiro T, Ross JC, Estepar RS, Lynch DA, Brehm JM, Andriole KP, Diaz AA, Khorasani R, D'Aco K, Sciurba FC, Silverman EK, Hatabu H, Rosas IO, Investigators CO. Lung volumes and emphysema in smokers with interstitial lung abnormalities. The New England journal of medicine. 2011; 364:897–906. [PubMed: 21388308]

6. Doyle TJ, Dellaripa PF, Batra K, Frits ML, Iannaccone CK, Hatabu H, Nishino M, Weinblatt ME, Ascherman DP, Washko GR, Hunninghake GM, Choi AM, Shadick NA, Rosas IO. Functional impact of a spectrum of interstitial lung abnormalities in rheumatoid arthritis. Chest. 2014; 146:41–50. [PubMed: 24305643]

7. Washko GR, Lynch DA, Matsuoka S, Ross JC, Umeoka S, Diaz A, Sciurba FC, Hunninghake GM, San Jose Estepar R, Silverman EK, Rosas IO, Hatabu H. Identification of early interstitial lung disease in smokers from the COPDGene Study. Academic radiology. 2010; 17:48–53. [PubMed: 19781963]

8. Jin GY, Lynch D, Chawla A, Garg K, Tammemagi MC, Sahin H, Misumi S, Kwon KS. Interstitial lung abnormalities in a CT lung cancer screening population: prevalence and progression rate. Radiology. 2013; 268:563–571. [PubMed: 23513242]

9. Bankier AA, De Maertelaer V, Keyzer C, Gevenois PA. Pulmonary emphysema: subjective visual grading versus objective quantification with macroscopic morphometry and thin-section CT densitometry. Radiology. 1999; 211:851–858. [PubMed: 10352615]

10. Xu Y, Sonka M, McLennan G, Guo J, Hoffman EA. MDCT-based 3-D texture classification of emphysema and early smoking related lung pathologies. IEEE transactions on medical imaging. 2006; 25:464–475. [PubMed: 16608061]

11. Matsuoka S, Yamashiro T, Matsushita S, Kotoku A, Fujikawa A, Yagihashi K, Nakajima Y. Quantitative CT evaluation in patients with combined pulmonary fibrosis and emphysema: correlation with pulmonary function. Academic radiology. 2015; 22:626–631. [PubMed: 25728361]

12. Iwasawa T, Asakura A, Sakai F, Kanauchi T, Gotoh T, Ogura T, Yazawa T, Nishimura J, Inoue T. Assessment of prognosis of patients with idiopathic pulmonary fibrosis by computer-aided analysis of CT images. Journal of thoracic imaging. 2009; 24:216–222. [PubMed: 19704326]

13. Best AC, Lynch AM, Bozic CM, Miller D, Grunwald GK, Lynch DA. Quantitative CT indexes in idiopathic pulmonary fibrosis: relationship with physiologic impairment. Radiology. 2003; 228:407–414. [PubMed: 12802000]

14. Rosas IO, Yao J, Avila NA, Chow CK, Gahl WA, Gochuico BR. Automated quantification of high-resolution CT scan findings in individuals at risk for pulmonary fibrosis. Chest. 2011; 140:1590–1597. [PubMed: 21622544]

15. Bartholmai BJ, Raghunath S, Karwoski RA, Moua T, Rajagopalan S, Maldonado F, Decker PA, Robb RA. Quantitative computed tomography imaging of interstitial lung diseases. Journal of thoracic imaging. 2013; 28:298–307. [PubMed: 23966094]

16. Mendoza CS, Washko GR, Ross JC, Diaz AA, Lynch DA, Crapo JD, Silverman EK, Acha B, Serrano C, Estepar RS. Emphysema Quantification in a Multi-Scanner Hrct Cohort Using Local Intensity Distributions. Proceedings/IEEE International Symposium on Biomedical Imaging: from nano to macro IEEE International Symposium on Biomedical Imaging. 2012:474–477.

17. Regan EA, Hokanson JE, Murphy JR, Make B, Lynch DA, Beaty TH, Curran-Everett D, Silverman EK, Crapo JD. Genetic epidemiology of COPD (COPDGene) study design. Copd. 2010; 7:32–43. [PubMed: 20214461]
18. Castaldi PJ, San Jose Estepar R, Mendoza CS, Hersh CP, Laird N, Crapo JD, Lynch DA, Silverman EK, Washko GR. Distinct quantitative computed tomography emphysema patterns are associated with physiology and function in smokers. American journal of respiratory and critical care medicine. 2013; 188:1083–1090. [PubMed: 23980521]
19. Ross JC, San Jose Estepar R, Kindlmann G, Diaz A, Westin CF, Silverman EK, Washko GR. Automatic lung lobe segmentation using particles, thin plate splines, and maximum a posteriori estimation. Medical image computing and computer-assisted intervention: MICCAI International Conference on Medical Image Computing and Computer-Assisted Intervention. 2010; 13:163–171.
20. Botev ZI, Grotowski JF, Kroese DP. Kernel density estimation via diffusion. The Annals of Statistics. 2010:2916–2957.
21. Snoek J, Larochelle H, Adams RP. Practical Bayesian Optimization of Machine Learning Algorithms. 2012:2951–2959.
22. Ley B, Collard HR, King TE Jr. Clinical course and prediction of survival in idiopathic pulmonary fibrosis. American journal of respiratory and critical care medicine. 2011; 183:431–440. [PubMed: 20935110]
23. Raghu G, Collard HR, Egan JJ, Martinez FJ, Behr J, Brown KK, Colby TV, Cordier JF, Flaherty KR, Lasky JA, Lynch DA, Ryu JH, Swigris JJ, Wells AU, Ancochea J, Bouros D, Carvalho C, Costabel U, Ebina M, Hansell DM, Johkoh T, Kim DS, King TE Jr, Kondoh Y, Myers J, Muller NL, Nicholson AG, Richeldi L, Selman M, Dudden RF, Griss BS, Protzko SL, Schunemann HJ. An official ATS/ERS/JRS/ALAT statement: idiopathic pulmonary fibrosis: evidence-based guidelines for diagnosis and management. American journal of respiratory and critical care medicine. 2011; 183:788–824. [PubMed: 21471066]
24. Best AC, Meng J, Lynch AM, Bozic CM, Miller D, Grunwald GK, Lynch DA. Idiopathic pulmonary fibrosis: physiologic tests, quantitative CT indexes, and CT visual scores as predictors of mortality. Radiology. 2008; 246:935–940. [PubMed: 18235106]
25. Coxson HO, Hogg JC, Mayo JR, Behzad H, Whittall KP, Schwartz DA, Hartley PG, Galvin JR, Wilson JS, Hunninghake GW. Quantification of idiopathic pulmonary fibrosis using computed tomography and histology. American journal of respiratory and critical care medicine. 1997; 155:1649–1656. [PubMed: 9154871]
26. Hartley PG, Galvin JR, Hunninghake GW, Merchant JA, Yagla SJ, Speakman SB, Schwartz DA. High-resolution CT-derived measures of lung density are valid indexes of interstitial lung disease. Journal of applied physiology. 1994; 76:271–277. [PubMed: 8175517]
27. Kim HJ, Brown MS, Chong D, Gjertson DW, Lu P, Coy H, Goldin JG. Comparison of the quantitative CT imaging biomarkers of idiopathic pulmonary fibrosis at baseline and early change with an interval of 7 months. Academic radiology. 2015; 22:70–80. [PubMed: 25262954]
28. Sverzellati N, Calabro E, Chetta A, Concari G, Larici AR, Mereu M, Cobelli R, De Filippo M, Zompatori M. Visual score and quantitative CT indices in pulmonary fibrosis: Relationship with physiologic impairment. La Radiologia medica. 2007; 112:1160–1172. [PubMed: 18193399]
29. Xu Y, van Beek EJ, Hwanjo Y, Guo J, McLennan G, Hoffman EA. Computer-aided classification of interstitial lung diseases via MDCT: 3D adaptive multiple feature method (3D AMFM). Academic radiology. 2006; 13:969–978. [PubMed: 16843849]

Rapid Communication Summary

In this study we describe a novel technique for the objective and fully automated detection of interstitial radiographic features on chest computed tomography scans. Our approach builds upon prior work by adding a distance measure from the pleural surface to a local histogram based analysis, in order to more accurately identify these features. In addition to the new approach, in this study we have also created a large database of over 30,000 unique radiographic labels, or training points, which we used, via a machine learning algorithm, to train the feature detector. Finally, using data from a previously reported visual analysis of over 2000 smokers not known to have interstitial lung disease, we have shown that our automated detector is able to accurately identify those subjects with visually identified interstitial lung abnormalities, with a c-statistic of 0.82. Prior work using purely densitometry based screening methods has been far less accurate, and there has been limited investigation into the role of an automated objective interstitial disease detector in individuals who are not at high risk for interstitial lung disease. Our study suggests that such an approach may have a role in the future as an automated screening tool to detect those individuals at highest risk for interstitial lung disease.

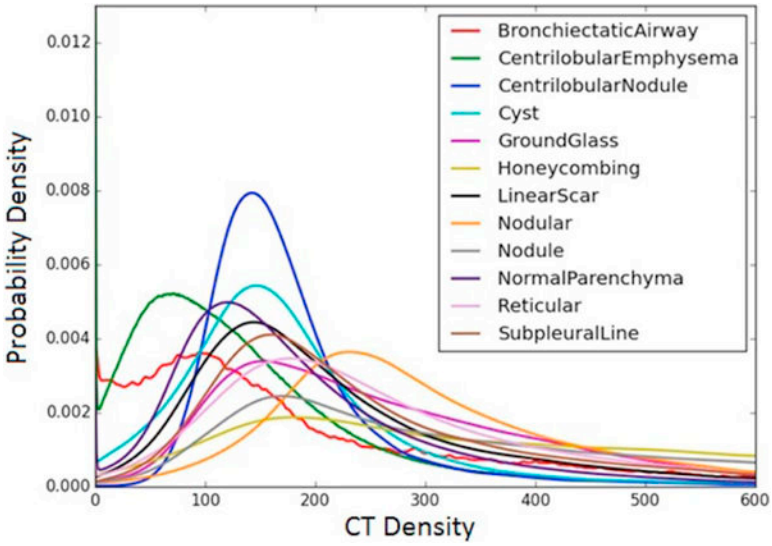

Figure 1.

Averaged kernel density estimates over the training samples for each radiographic type. Each kernel density estimate approximates the probability density function over CT density values in the training patch.

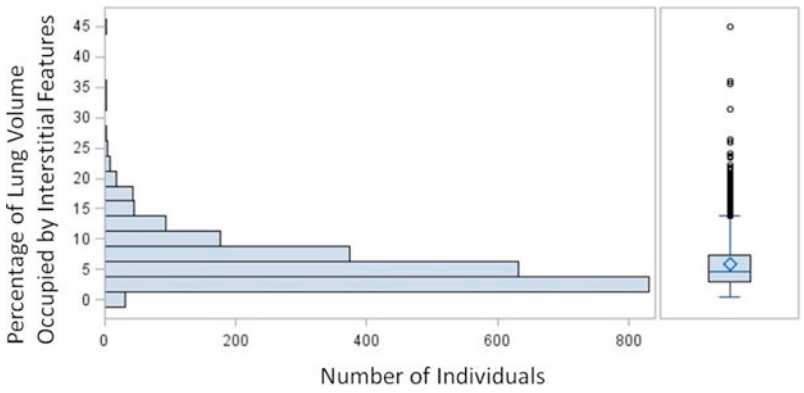

Figure 2.

Cohort distribution of the percentage of objective interstitial features within each individual subject's CT scan

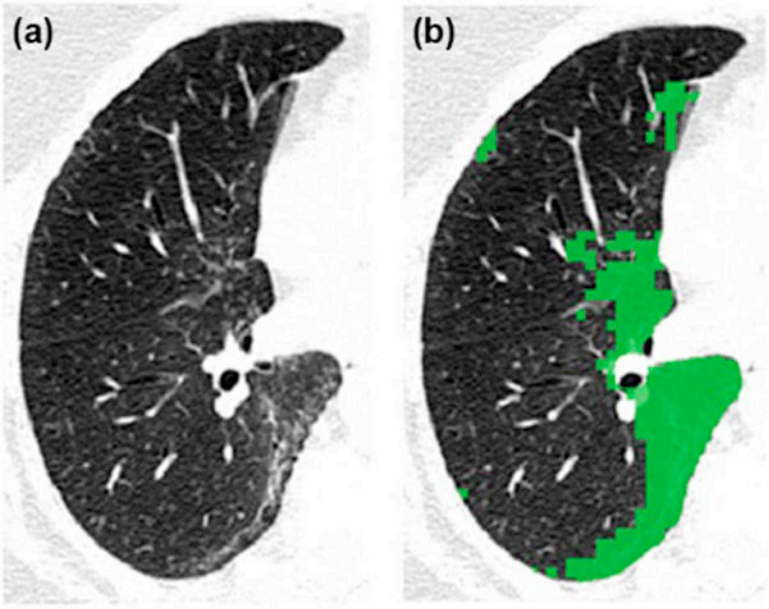

Figure 3.
HRCT (A) with overlay of objectively defined interstitial lung features (B).

Table 1

Cohort Characteristics

Clinical	
Age (years) - mean (std dev)	61.0 (9.31)
Sex - % female (n)	48.7 (1099)
Race - % black (n)	25.3 (570)
BMI - mean (std dev)	28.5 (6.20)
Pack Years - mean (std dev)	45.4 (25.28)
Current Smoking - % (n)	44.4 (1001)
FEV1 (% predicted) - mean (std dev)	74.7 (27.01)
MMRC (score) - mean (std dev)	1.39 (1.46)
Visual	
% with interstitial lung abnormalities present visually (n)	6.91 (156)